https://doi.org/10.1016/j.jbiomech.2020.110154

Assessment of trunk muscle activation and intervertebral load in adolescent idiopathic scoliosis by musculoskeletal modelling approach

Noemi Barba [a], Dominika Ignasiak [b], Tomaso Maria Tobia Villa [a], Fabio Galbusera [c], Tito Bassani [c]

[a] Department of Chemistry, Materials and Chemical Engineering "Giulio Natta", Politecnico di Milano, Milan, Italy

[b] Institute for Biomechanics, ETH Zurich, Zurich, Switzerland

[c] IRCCS Istituto Ortopedico Galeazzi, Milan, Italy. LABS - Laboratory of Biological Structures Mechanics

Keywords

Musculoskeletal modelling; Scoliosis; Spine; Subject-specific; AnyBody

Corresponding author

Tito Bassani - IRCCS Istituto Ortopedico Galeazzi LABS – Laboratory of Biological Structures Mechanics, via R. Galeazzi 4, 20161 Milan, Italy.

E-mail address: tito.bassani@grupposandonato.it

Abstract

Adolescent idiopathic scoliosis (AIS) is a three-dimensional deformity of the spine, the aetiology and pathogenesis of which are poorly understood. Unfortunately, biomechanical data describing trunk muscle activation and intervertebral load, which can contribute to understanding the pathomechanics of the AIS spine, cannot be measured in vivo due to the invasiveness of the procedures. The present study provides the biomechanical characterization of the spinal loads in scoliotic subjects by exploiting musculoskeletal modelling approach, allowing for calculating biomechanical measures in an assigned posture. A spine model with articulated ribcage previously developed in AnyBody software was applied. The predicted outcomes were evaluated in the upright posture, depending on scoliosis severity and curve type, in a population of 132 scoliotic subjects with mild, moderate, and severe scoliosis. Radiographic based three dimensional reconstruction of vertebral orientations and scaling of body segments and trunk muscle cross-section area guaranteed geometrical subject-specificity. Validation analysis supporting the application of the model was performed. Trunk muscles were found more activated in the convex side of the scoliotic curve, in agreement with reference in vivo measurements,

with progressive increase with scoliosis severity. The intervertebral lateral shear was found positively correlated with the severity of the scoliosis, demonstrating that the transferred load is not a priori orthogonal to vertebral endplate in the frontal plane, and thus questioning the assumption of the 'follower load' approach in case of experimental or computational study on the scoliotic spine. The study opens the way for the subject-specific characterization of scoliosis in assigned loading and motion conditions.

1. Introduction

Adolescent idiopathic scoliosis (AIS) is a three-dimensional deformity of the spine occurring in the general population with prevalence between 2 and 3% (Fong et al., 2010; Weinstein et al., 2008), the aetiology and pathogenesis of which are poorly understood (de Sèze and Cugy, 2012; Schlösser et al., 2014). In the frontal plane, scoliosis exhibits a lateral deviation of the spine with one or more curves, the severity of which is measured on radiographic images by the Cobb angle (Nnadi and Fairbank, 2010) (Fig. 1a). Several methods have been proposed to differentiate the scoliosis typology depending on number and extent of the curves and spine level (Ovadia, 2013). The most popular and comprehensive is the Lenke classification (Lenke et al., 2001), which accounts for six different types.

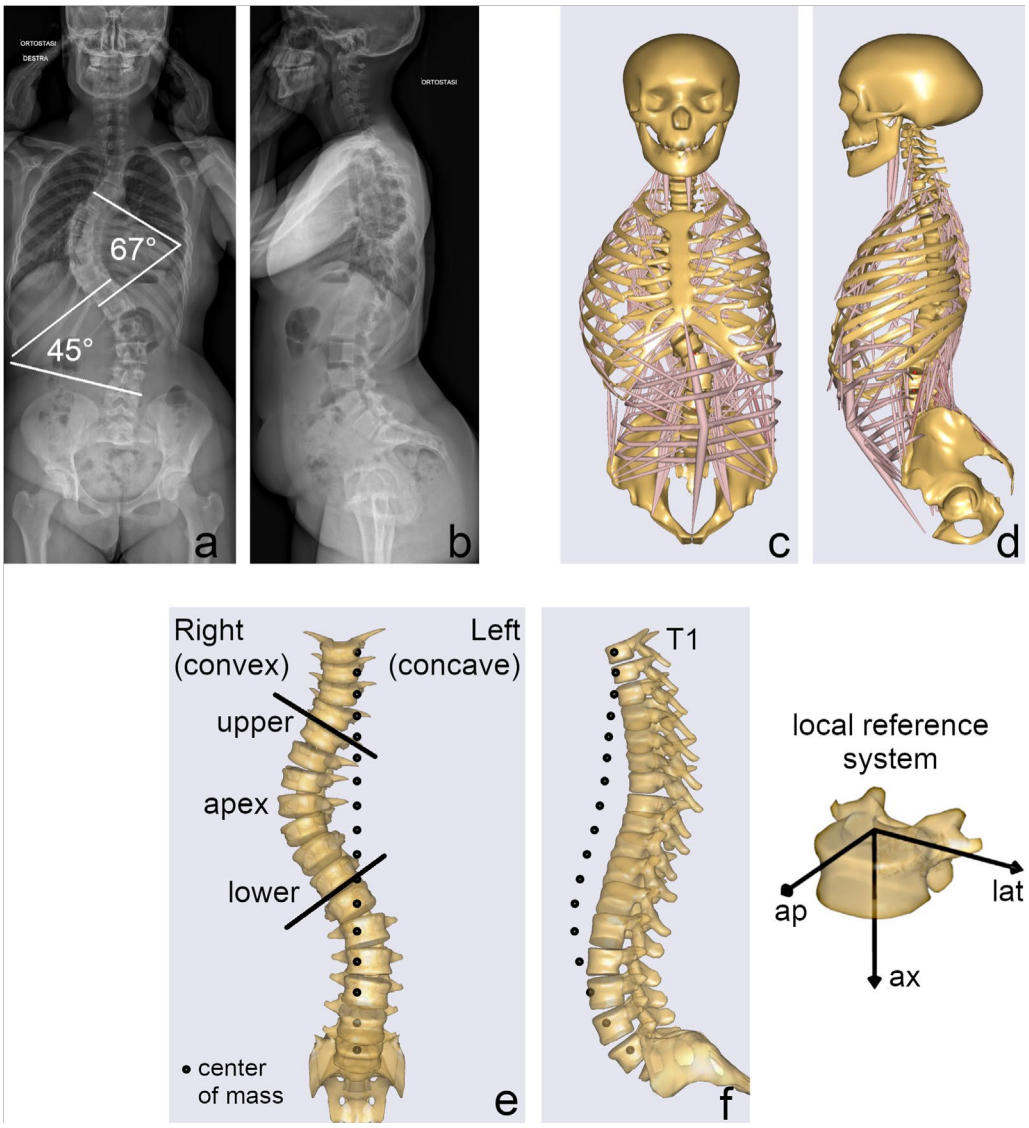

Fig. 1. Frontal and lateral radiographic images of one subject (a,b) and corresponding musculoskeletal model (c,d), also presented highlighting the primary scoliotic curve (apex, upper and lower vertebrae) with muscles and ribcage not shown (e,f) to better illustrate the replication of the spine alignment and the position of the centers of mass.

Investigating the relationship between scoliosis and biomechanical measures such as muscle activation and intervertebral forces could provide valuable information for the understanding of the pathomechanics of the AIS spine. Unfortunately, these measures cannot be obtained in vivo due to the invasiveness of the measurement procedures (i.e., intramuscular EMG, and intradiscal pressure or implant-based vertebral load measurements). An alternative strategy is represented by computational simulation based on musculoskeletal modelling approach, which allows calculating the biomechanical loads in assigned kinematic conditions by the means of inverse dynamic analysis (Dreischarf et al., 2016). In this regard, an investigation of subjects with mild scoliosis has been recently performed in OpenSim software to evaluate the effects of carrying loads on spinal compressive forces (Schmid et al., 2020). It is worth noting that idiopathic scoliosis is a multifactorial condition including genetic factors,

growth effects, and structural causes. Its development is often referred to as a “vicious cycle” in which the spinal curvature provides asymmetric loads, which provide asymmetric growth, which can affect spinal curvature again (Stokes et al., 1996). Although the musculoskeletal modelling approach requires an imposed initial anatomical deformity to allow calculating potential muscle asymmetries, thus preventing the study of the onset of scoliosis, the computed loads can be exploited to simulate postural and motion conditions as well as to predict their impact on the risk of curve progression. Modelpredicted loads might provide reference values dictating design of medical devices such as spinal implants used for correcting deformity, and patient-specific simulations have a potential to guide in the future treatment and rehabilitation tailored to a particular curve type and severity.

The main aim of this study was to investigate the effects of scoliosis severity and type on the patterns of trunk muscle activation and resultant spinal loads, by musculoskeletal simulations of realistic (patient-specific) spine alignments representing a range of mild, moderate and severe cases. We hypothesized that the leftto-right imbalance in muscle activity, as well as lateral spinal forces increase with scoliotic curve severity, and depend on the curvature characteristics (such as: curve apex, or upper and lower end). To address this aim, a previously established and validated musculoskeletal model of the thoracolumbar spine with articulated ribcage (Ignasiak et al., 2016a,b) developed in AnyBody modeling software (AnyBody Technology, Denmark) was modified to allow representation of scoliotic spinal alignments. Validation of the modified model application to simulate scoliotic alignments was performed by comparing the predicted muscle activities with in vivo data available in literature and corresponding values predicted in the previous modelling study by Schmid et al., in which a different model and simulation software were used. Finally, the upright standing simulations of 132 spinal alignments corresponding to AIS subjects with various degree of deformity severity were performed, and resulting muscle and spinal forces were analyzed in relation to curve characteristics.

2. Methods

2.1. Subjects’ dataset

A dataset of 132 AIS subjects (age ranging from 8 to 18 years) with mild (Cobb angle ranging from 10 to 25), moderate (2545), and severe (>45) scoliosis, acquired and evaluated in a previous clinical study (Bassani et al., 2019) was exploited (Table1). The subjects underwent radiological examination in orthostatic position, with arms raised and fingertips on cheekbones, by EOS Imaging System (EOS Imaging, France), providing the simultaneous acquisition of the frontal and lateral plane images (Fig. 1a,b). Age, weight, height, and classification of scoliosis according to Lenke type (Lenke et al., 2001) were available. The images were processed by sterEOS software allowing for the reconstruction of the

3D orientations of the thoracolumbar vertebrae (from T1 to L5) and the pelvis in the anatomical planes, as well as for the identification of the scoliotic curves with corresponding Cobb angle (Illes and Somoskeoy, 2012; Somoskeoy et al., 2012).

2.2. Characterization by musculoskeletal modelling

A thoracolumbar spine model with articulated ribcage, previously developed and validated in AnyBody software by (Ignasiak et al., 2016a,b), was applied (Fig. 1c,d). In this model, the pelvis is constrained to the ground and rigidly connected to the sacrum. The vertebral segments are connected by spherical joints (from cervical to lumbar region and between L5 and sacrum), whereas single compound revolute joints connect ribs to vertebrae from T1 to T10. The sternum is connected to ribs by 6 degrees of freedom costo-sternal articulations representing deformable costal cartilages and synovial joints. An additional spherical joint connecting the mediocranial limit of the sternum to T1 segment, not representing any anatomical structure, is defined in the present work to allow for the rearrangement of the ribcage as explained below. Software version 6.1 was used in the present study.

The subject-specific spine alignment was replicated by setting the orientation of the sacrum in the lateral plane and the rotation of the intervertebral joints from T1 to L5 (Fig. 1e,f). After that, the following consecutive steps were performed to adjust the orientation of the sternum and ribs segments to obtain an appropriate rearrangement of the ribcage: i) T1-sternum joint was rotated to align the craniocaudal axis of the sternum with the line connecting the center of T1 and that of the sacral upper endplate in the frontal plane; ii) orientation of the joint nodes connecting ribs to vertebrae were counter-rotated with respect to vertebral orientation, thus obtaining the rearrangement of ribs orientation according to default not-scoliotic model; iii) additional rotation of the nodes was imposed to minimize the distance between ribs and sternum attachment points in the frontal and axial plane.

Applying joint rotation angles modifies the orientation of the connected body segment, and thus the position of the segment's elements with respect to the center of rotation. As a result, the changes in the position of the muscle insertion points that are more far from the joint center, such as those of the abdominal muscles in the thoracolumbar section, can provide non-rational arrangements of the abdominal structure. Therefore, in order to preserve the original abdominal setting of the default notscoliotic model, the position of the attachment points of obliquus externum, obliquus internum, quadratus lumborum, iliocostalis and longissimus muscle defined in T11 and T12 segments were systematically adjusted by counter-rotating with respect to the joint rotation angles. The model was scaled by subject's weight and height using default length-mass-fat approach. Joint moments, representing the stiffness-related contribution of passive elements such as ligaments and facet joints, were assumed as zero to replicate neutral upright standing position. Due to the absence of reference in

vivo data, the centers of mass of the body segments were repositioned to preserve the original placement defined in the default not-scoliotic model (Fig. 1e,f) (Ignasiak et al., 2016a,b).

Since AIS has been reported as associated with side-to-side asymmetries in spinal muscle geometry (Zapata et al., 2015; Zoabli et al., 2007), the physiological cross-section area (PCSA) of left and right erector spinae (ES, characterized by 44 fascicles in each side), multifidus (MF, 55 fascicles), psoas major (11 fascicles) and quadratus lumborum (5 fascicles), was scaled accounting for reference values acquired in scoliotic subjects for four age ranges (8–10, 11–13, 14–16, and 17–20 years), reported for respective sides (Been et al., 2018). Specifically, for each spine level from T1 to L5, the cumulative PCSA was obtained separately for right and left side by summing the PCSAs of the individual fascicles crossing the respective vertebral mid-plane. The cumulative PCSA was scaled to replicate the reference scoliotic value and equally subdivided in the muscle fascicles. Since reference values were provided only for levels from L3 to sacrum (Been et al., 2018), the average of reference values among those levels was calculated and the cumulative PCSA at another level was set as guaranteeing the same relation between level and average L3-sacrum as that provided in the default not-scoliotic model.

The head and neck segments were reoriented to preserve horizontal gaze. Two external forces (5% of subject's weight each) were applied at T1 level, 10 and 7 cm laterally and frontally to vertebral centroid, respectively, to simulate the load of the raised arms. Muscle co-activation in maintaining the upright posture was simulated by imposing lower bound activation threshold of 3% for ES and MF muscle fascicles. Such level was selected as the minimum value preventing near zero activation levels for all the simulations. Inverse static analyses were run to calculate muscle activation and intersegmental reaction forces in the assigned standing posture. The setting steps and simulations were run in batch process using custom routines written in MATLAB (MathWorks Inc., Natick, MA, USA). The routines guaranteed the following sequence of automatic tasks: import the subject-specific parameters from data sheet, assign the corresponding values in the AnyBody script files defining the model, launch the simulation steps, save the model outcomes in MATLAB format for the comparison of the results.

	scoliosis severity		
	mild	moderate	severe
subjects (N = 132)	36 (27%)	69 (52%)	27 (21%)
age [years]	14(2)	14(2)	14(2)
weight [kg]	47(8)	51(10)	54(10)
height [cm]	160(11)	161(11)	162(9)
Cobb angle [°]	20(3)	33(6)	57(7)
subjects with 1 and 2 curves	20/16	3/66	0/27
right and left convexity of the primary curve	16/20	39/30	23/4

Table 1. Values describing the evaluated population of AIS subjects depending on scoliosis severity and reported as number of individuals or mean(SD).

2.3. Model validation

The modified model allowing for the characterization of scoliosis was validated by comparing the predicted values of ES muscle activation to in vivo measurements available from the literature (obtained by surface-EMG in subjects with Cobb angle ranging from 10 to 30) (Cheung et al., 2005; Kwok et al., 2015), and to corresponding values predicted by Schmid et al. by exploiting musculoskeletal modelling developed in OpenSim software (Schmid et al., 2020). Specifically, the activation ratio between the convex and concave side of the scoliotic curve was compared. In order to perform an accurate comparison, only the subjects with Cobb angle lower than 30 and characterized by thoracic or thoracolumbar primary scoliotic curve (i.e., the most severe in case of two curves) were taken into account. The cumulative muscle activation was computed at each spine level on the right and left side by summing the activations of the individual fascicles (ranging from 0 to 1) crossing the respective vertebral mid-plane. The average value in the thoracic (T1-T12) and lumbar (L1-L5) region, as well as the specific value at the apex, upper and lower vertebral ends of the curve (Fig. 1e) were compared. The intersegmental forces were not compared due to the lack of in vivo studies reporting on functional spinal loading (e.g., segmental compressive forces or intradiscal pressure in upright standing conditions) in AIS patients.

2.4. Relationship between biomechanical measures and scoliosis

The activation of ES and MF muscle was evaluated, accounting for all subjects, in the primary scoliotic curve at apex, upper and lower end vertebral levels. The cumulative muscle activation was computed at each spine level. Similar to that performed in the validation analysis, the imbalance in muscle

activation was evaluated between the convex and concave side. In this case, a normalized activity ratio calculated as (convex concave)/(convex + concave), was considered. This parameter provides values near zero in correspondence of balanced activation, and positive and negative values (ranging from 0 to ± 1) in case of larger activation in the convex and concave side, respectively. Such an approach was chosen because providing values distributions and range that are more homogeneous and comparable (also in statistical perspective) with respect to computing convex/concave ratio, which in case of more severe scoliosis (exceeding 30) can provide considerably larger and scattered values. The changes in muscle activation were evaluated depending on the scoliosis severity and spine level.

The intersegmental reaction force, F, was evaluated at the apex, upper and lower end levels, expressed in the local reference system of the vertebra: anteroposterior and lateral shear (Fap and Flat, respectively) and axial compression force (Fax) (Fig. 1). Since expected as the most affected by lateral deviations of the spine in the frontal plane which characterize scoliosis, the absolute value of Flat was put in relation with scoliosis severity and Lenke type. The strength of the relation was evaluated by Pearson correlation coefficient or Spearman rank in case of non-normal distribution of data. In order to evaluate how scoliosis affects the orientation of the transferred intervertebral load, the distribution of the components of F (Fap, Fax, and Flat) was assessed in relation to scoliosis severity and spine level. Each component was normalized as the ratio between its absolute value and the sum of the absolute values of the three.

2.5. Statistical analysis

The significance of differences in the normalized activity ratio of ES and MS muscle, as well as in the absolute value of Flat, were tested depending on two factors: scoliosis severity (mild, moderate, and severe), and vertebral level in the scoliotic curve (apex, upper and lower end). Two-way ANOVA was applied if the tested subgroups were verified as normally distributed (Bassani and Galbusera, 2020). If that condition was not satisfied, each factor was tested separately according to one-way ANOVA or KruskalWallis test. In case of overall significance, post-hoc pairwise comparisons were performed exploiting the Tukey-Kramer approach. The significance of Pearson or Spearman correlation coefficient in being statistically different from zero was tested according to two-tailed t test or permutation distribution test, respectively. All the tests assumed 0.05 as significance level. The analyses were performed in MATLAB software.

3. Results

3.1. Model validation

The subgroup of subjects with Cobb angle < 30 and thoracic or thoracolumbar primary scoliotic curve (63 subjects) was considered. Overall, the predicted activation ratio of ES muscle was found comparable to in vivo measurements and values predicted by Schmid et al. (Fig. 2). Values larger than one, indicating higher activation in the side of the convexity of the scoliotic curve, were found in the thoracic region (1.53(0.91) and 1.14(0.46), as mean(SD), for subjects with thoracic and thoracolumbar curve, respectively) and lumbar region (1.34(0.47) and 1.21(0.33)), as well as at the apex (1.51(0.83)) and upper and lower ends (1.41(0.91) and 1.29 (0.59)) of the curve. The computed values were found very similar to those previously predicted, whereas the in vivo measurements provided lower values in the lumbar region when considering thoracolumbar curves, and at the upper end of the curve.

3.2. Relationship between biomechanical measures and scoliosis

Examples of the prediction of muscle activation and intersegmental load (F) are presented in Fig. 3 (depicted by markers plots and vectors, respectively) for representative subjects with mild, moderate and severe scoliosis. In these cases, the normalized activity ratio of ES and MF is determined as (Left Right)/(Left + Right) muscle activity, allowing for a direct representation of its distribution along the vertebral levels. The normalized muscle activity ratios were found dependent on spine alignment, with increasingly greater values predicted for the moderate and severe cases. The direction of F was in general orthogonal to the vertebral endplate in the lateral plane, but was more laterally oriented in the frontal plane for the greater scoliosis severities.

When considering all subjects, the results are provided by heatmap plots reporting the mean values (or specific value in case of conditions with single subject) calculated in the subgroups characterized by specific spine level (for apex, upper and lower end vertebra) and Cobb angle (Fig. 4 and Fig. 5d,e,f). The number of subjects within each subgroup is reported in Fig. 4a,b,c. Subgroups including only a single subject are displayed as well, in order to provide a broader scope of results. Overall, ES and MF were found to be progressively more activated in the convex side (yellow to red shades of color) depending on increase in scoliosis severity, and generally in the spine levels from T7 to T11 for the apex (Fig. 4a,d), T6-T8 for upper end (Fig. 4b,e), and T10-L1 for lower end (Fig. 4c,f). The mean value was higher for severe scoliosis (ranging from 0.24 to 0.35 and from 0.04 to 0.33 for ES and MF, respectively) compared to mild (0.03–0.08, 0.03–0.14) and moderate (0.15–0.23, 0.01–0.23) conditions, and larger values were generally found at upper and lower end compared to apex (Table2).

The lateral component of the intersegmental load (Flat) correlated strongly with scoliosis severity at lower and upper end (0.79 and 0.69, Fig. 5b,c) and moderately at apex (0.57, Fig. 5a), with similar linear relationship among the Lenke types. The heatmap plots highlighted that greatest values of Flat were generally found at the spine levels which presented the greatest muscle activation (Fig. 5d-f). The mean value ranged from 183 to 250 N for severe scoliosis, and was lower in moderate (70–118 N) and mild (27–55 N) condition (Table2). Lower values were found at the upper end compared to the other curve levels. The evaluation of the distribution of the components of F (F_{ap}, F_{ax}, and F_{lat}) confirmed the progressive increase of Flat depending on the scoliosis severity (black bars in Fig. 6), and showed that the anteroposterior shear, Fap, is in general negligible with respect to the axial compression, F_{ax}, in all the considered conditions (light and dark grey bars, respectively).

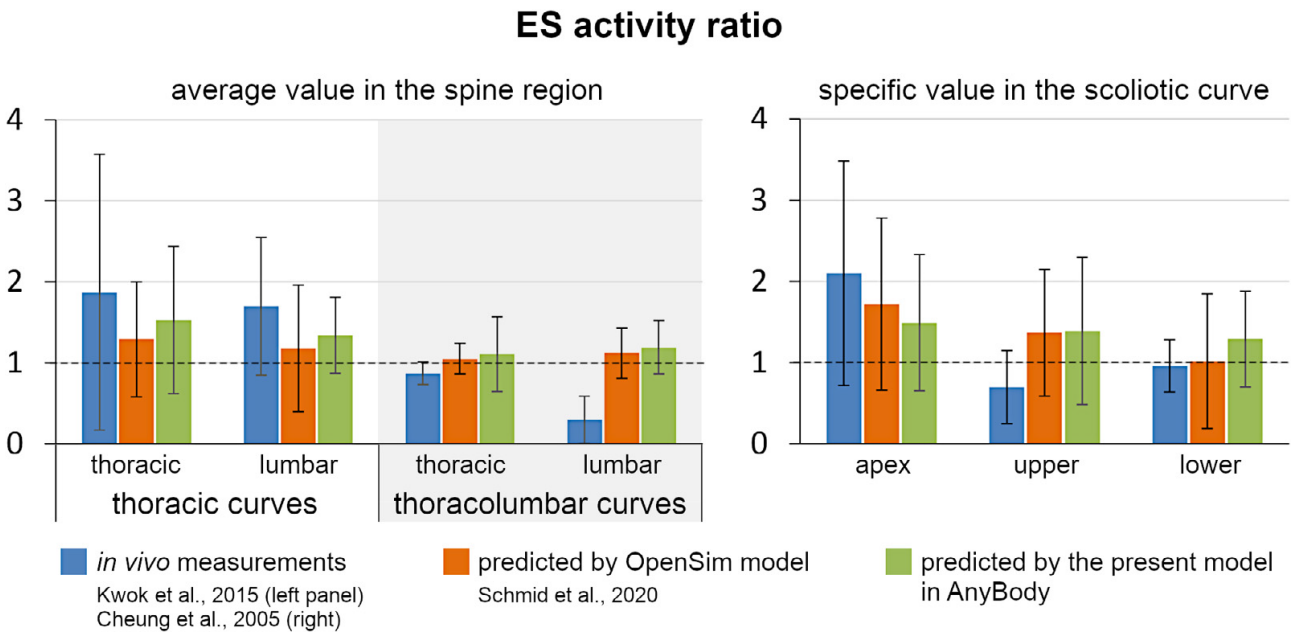

Fig. 2. Convex to concave ratio for erector spinae (ES) muscle activity provided as mean ± SD: average value in the thoracic and lumbar regions for subjects with thoracic or thoracolumbar primary curve (left panel), and specific value at the apex and the upper and lower ends of the curve (right panel). Comparison between in vivo measurements provided by (Kwok et al., 2015) (left panel) and by (Cheung et al., 2005) (right panel), and results predicted by (Schmid et al., 2020) and by the present model.

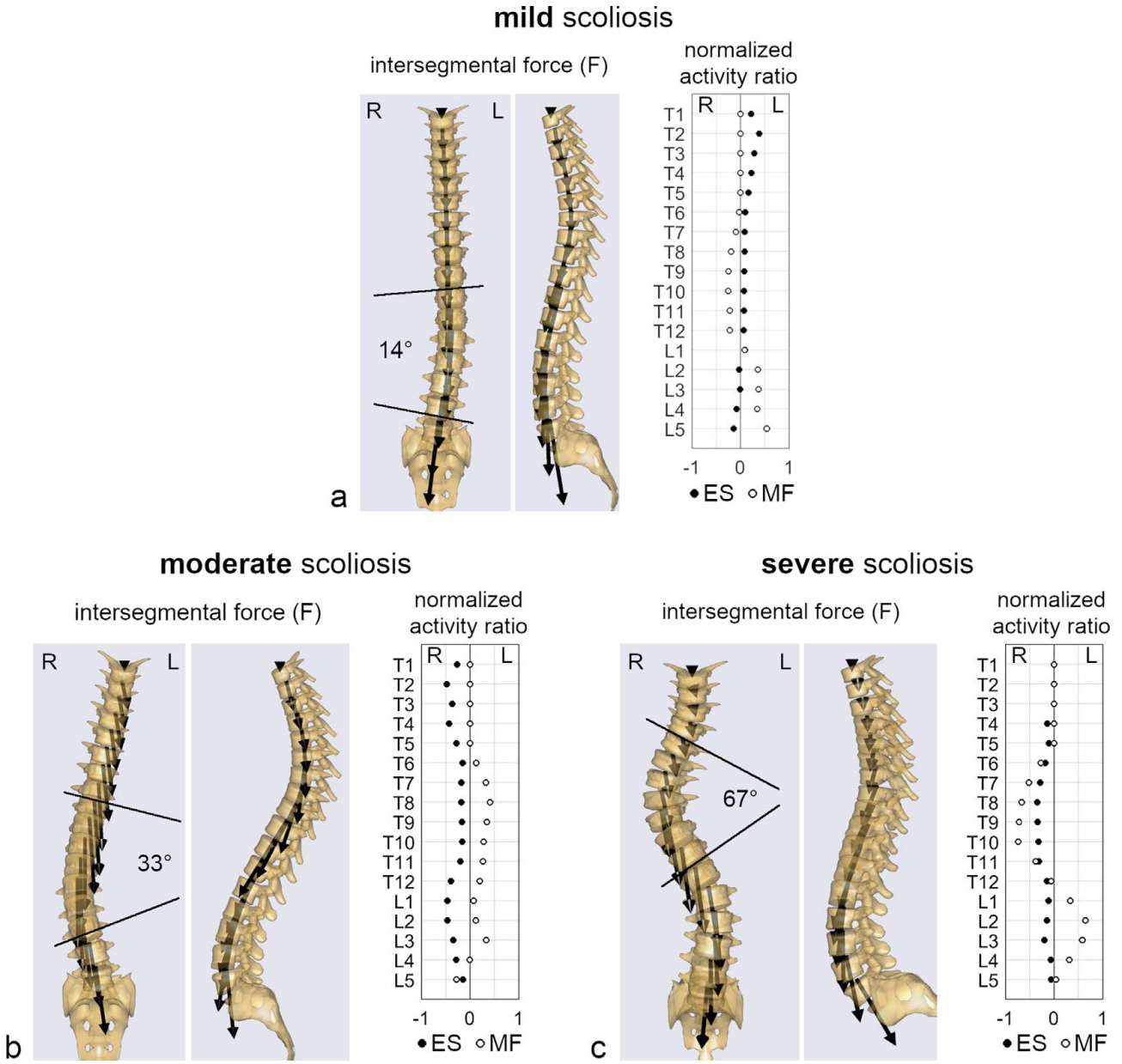

Fig. 3. Example of predicted intersegmental load, F, and normalized activity ratio for erector spinae (ES) and multifidus (MF) muscle at spine levels from T1 to L5, in subjects with mild (panel a), moderate (b) and severe (c) scoliosis. The normalized activity ratio is calculated as (Left-Right)/(Left + Right).

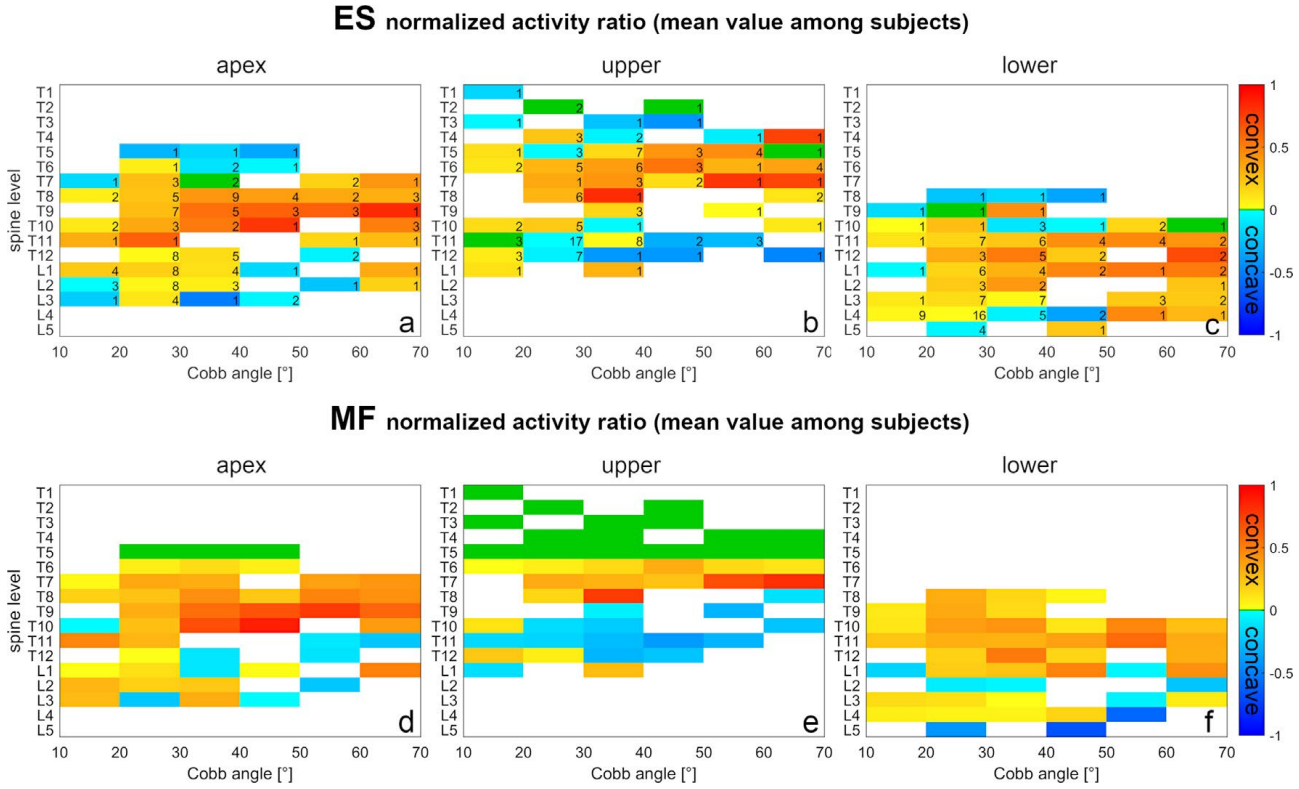

Fig. 4. Heatmap plots depicting the mean value of the normalized activity ratio for erector spinae (ES) and multifidus (MF) muscle, calculated among subjects in correspondence of spine level and scoliosis severity at apex (a,d), upper end (b,e) and lower end (c,f) vertebra of the scoliotic curve. For example, the first cell (colored in light blue) in correspondence of T7 and 10-20 in (a), depicts the mean value among those subjects with Cobb angle in that range and curve apex in T7. The number of evaluated subjects for each spine level/Cobb angle condition is reported in the corresponding cell in the plots of the first row (a,b,c). The white spaces indicate absence of subjects in the considered condition. The normalized ratio is calculated as (convex side – concave side)/(convex side + concave side). The green color depicts the zero value.

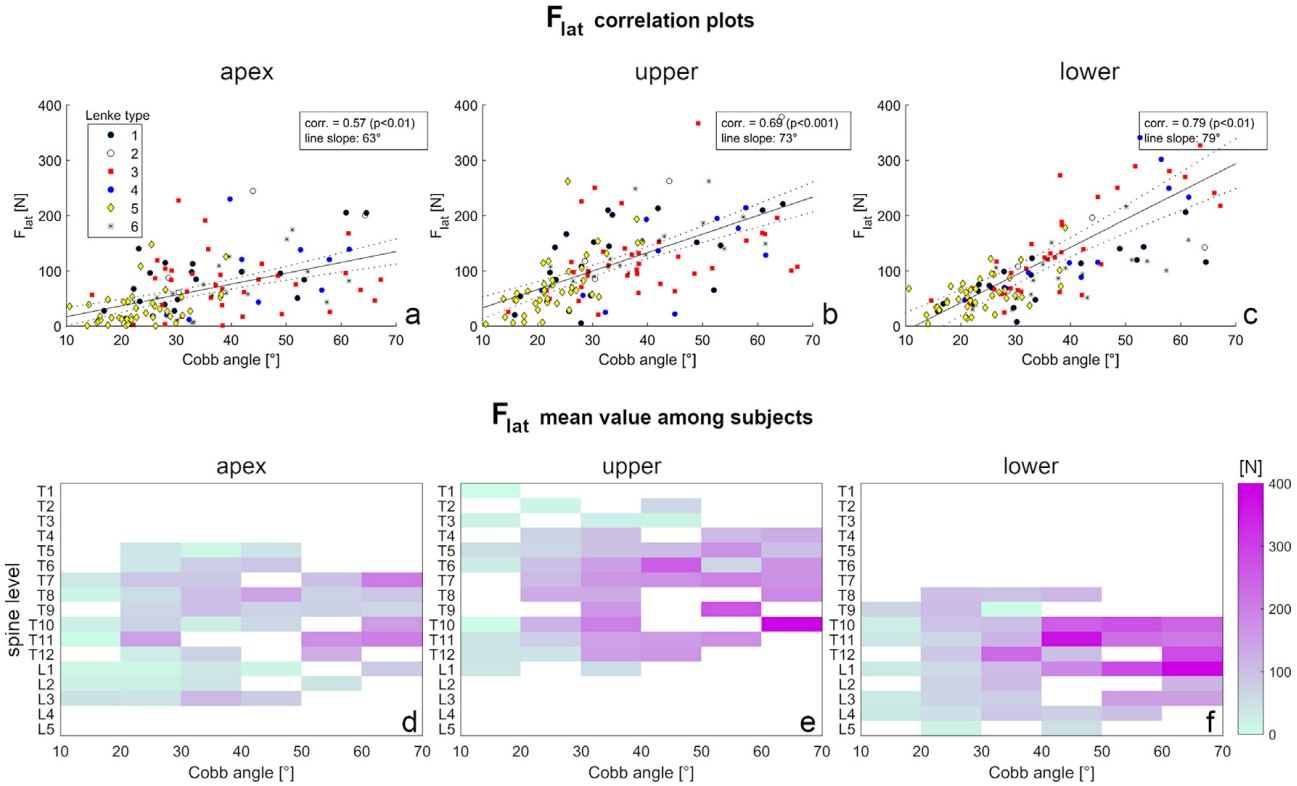

Fig. 5. Upper row: scatter correlation plots depicting the relation between lateral shear (Flat, absolute value) and scoliosis severity, depending on Lenke type, at apex (a), upper end (b) and lower end (c) vertebra of the scoliotic curve. For each subplot, the regression line with 95% confidence interval, the correlation coefficient (with statistical significance of being different from zero) and the line slope are reported. Lower row: heatmap plots depicting the mean value of Flat, calculated among subjects in correspondence of spine level and scoliosis severity at apex (d), upper end (e) and lower end (f) vertebra of the scoliotic curve. The white spaces indicate absence of subjects in the considered level/degrees condition.

		ES normalized activity ratio			
		scoliosis severity			
		mild (A)	moderate (B)	severe (C)	significance
curve level	apex (I)	0.03(0.18)	0.15(0.31)	0.24(0.39)	A vs C
	upper (II)	0.08(0.15)	0.23(0.3)	0.34(0.31)	A vs B,C
	lower (III)	0.05(0.14)	0.16(0.28)	0.35(0.23)	C vs A,B
	significance	II vs I,III	II vs I,III	II vs I,III	
		MF normalized activity ratio			
		scoliosis severity			
		mild (A)	moderate (B)	severe (C)	significance
curve level	apex (I)	−0.03(0.23)	−0.01(0.26)	0.04(0.33)	–
	upper (II)	0.14(0.24)	0.23(0.33)	0.33(0.37)	–
	lower (III)	0.06(0.27)	0.18(0.31)	0.23(0.38)	–
	significance	I vs II	I vs II,III	I vs II	
		F_{lat}			
		scoliosis severity			
		mild (A)	moderate (B)	severe (C)	significance
curve level	apex (I)	55(33)	118(61)	183(81)	all pairs
	upper (II)	27(30)	70(54)	103(55)	all pairs
	lower (III)	45(20)	98(58)	250(190)	all pairs
	significance	II vs I,III	II vs I,III	II vs I,III	

-. indicates no significances found.

Table 2. Mean (SD) values for normalized activity ratio of ES and MF muscle, and for lateral shear (Flat), depending on scoliosis severity and vertebral level in the scoliotic curve. Statistical significance of the pairwise post-hoc comparisons is reported as well.

4. Discussion

The present study investigated the relationships between model-predicted biomechanical measures (trunk muscle activation and intervertebral forces) and scoliosis characteristics in static upright posture (Fig. 1), using a previously developed musculoskeletal (AnyBody) model of the thoracolumbar spine with appropriate modifications. The modified model allowing for characterizing scoliosis was validated by comparing the activation ratio of ES muscle to in vivo measurements based on EMG (Cheung et al., 2005; Kwok et al., 2015) and corresponding values predicted by Schmid et al. by a recently developed model based on OpenSim software (Schmid et al., 2020). The analysis, performed for subjects with mild and moderate scoliosis (<30), provided comparable values and supported the suitability of the present model, confirming that the muscle activation is generally larger in the convex side of the scoliotic curve (activity ratio > 1, Fig. 2). Interestingly, the analysis also confirmed that the musculoskeletal models predict in general a more balanced activation compared to in vivo measurements, in particular in the lumbar region for thoracolumbar curves.

As regards the relationship between ES and MF muscle activation and scoliosis severity, the evaluation of all subjects (mild, moderate and severe cases) revealed a progressive imbalance (increase in the convex side) dependent on curve severity (Fig. 4). This relation can be observed in detail in the examples illustrated in Fig. 3, in which the activation ratio shows to be dependent on spine alignment as well as on curve severity. Overall, the increase was larger and statistically significant for ES, and lower for MF (Table2). Moreover, for both muscles the convex side resulted significantly more activated at the ends of the curve compared to apex. Similar differences were found by evaluating the intersegmental reaction forces. As illustrated in the examples provided (Fig. 3, frontal plane view), the lateral shear component of the force vector increased with scoliosis severity. Overall, Flat resulted strongly correlated with the scoliosis severity (Fig. 5a-c), and the increase from mild to severe scoliosis condition was significant at each curve level (Table2). Higher values were found at apex and lower end compared to upper end, due to the increase of transferred body weight load from the upper to lower spine levels.

Interestingly, differently from that observed in the frontal plane, the orientation of the force vector resulted orthogonal to the vertebral endplates in the lateral plane (Fig. 3). This finding is better illustrated by comparing the distribution of the force components in relation to scoliosis severity and spine level (Fig. 6), showing that the anteroposterior shear, Fap, was in general negligible with respect to the axial compression, Fax, in all the considered conditions. This outcome questions the assumption of the 'follower load' approach in case of experimental or computational study on the scoliotic spine (Buttermann and Beaubien, 2008; Hachem et al., 2017; Stokes and Gardner-Morse, 2004). This method consists indeed in applying a compressive pre-load to vertebral bodies avoiding any intervertebral

rotation (Patwardhan et al., 1999), and is nowadays applied in many in vitro experiments and finite element analyses to mimic the in vivo situation, most commonly for non-scoliotic spines (Dreischarf et al., 2010; Panjabi et al., 2007; Rohlmann et al., 2001; Rohlmann et al., 2009; Wilke et al., 2003). Accordingly, assuming purely orthogonal load when investigating scoliosis conditions, neglecting the contribution of the lateral shear component, should be considered as an intrinsic limitation.

Structural peculiarities and strengths and limitations of using musculoskeletal modelling approach for the characterization of the human spine have been extensively reviewed and discussed previously (Dreischarf et al., 2016; Dao, 2016; Bassani and Galbusera, 2018). In the context of the present study, the following limitations should be mentioned. The validation was performed only for mild and moderate scoliosis (<30), due to the lack of experimental data characterizing more severe cases, and was based only on comparison of ES muscle activations to surface EMG signals. As regards the model structure, the pelvis was constrained to the ground, neglecting lower limbs and arms, as well as sacroiliac mobility. However, this limitation is expected to potentially affect the activation of the psoas and abdominal muscle in upright posture and not that of ES and MF, as well as the prediction of the intervertebral forces. In the thoracolumbar segments, the position of several muscle insertion points was systematically adjusted to preserve the original abdominal structure.

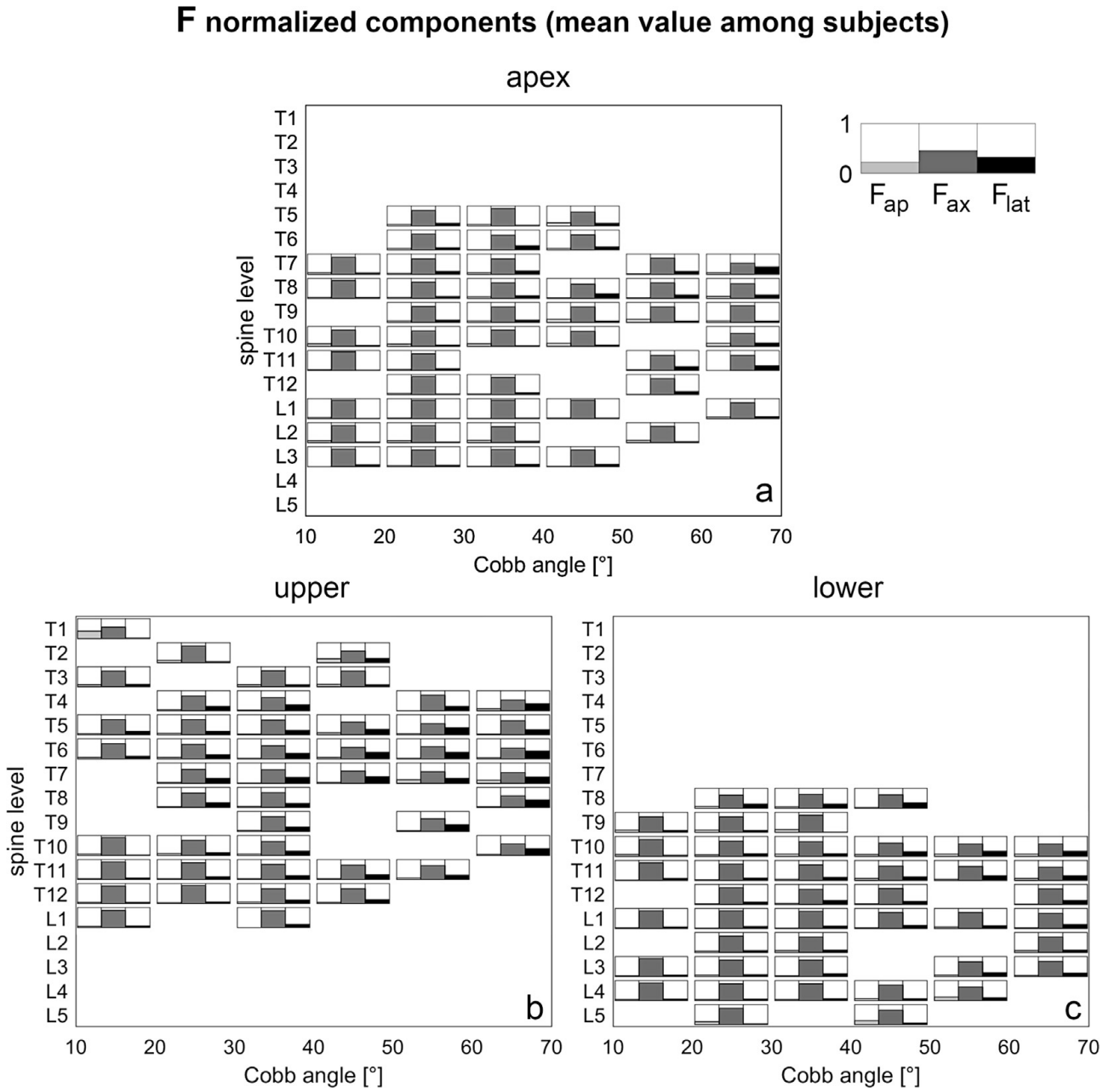

Fig. 6. Bar plots depicting the mean value of the normalized components of the intersegmental load F (F_{ap}, F_{ax}, and F_{lat}, see Fig. 3), calculated among subjects in correspondence of spine level and scoliosis severity at apex (a), upper end (b) and lower end (c) vertebra of the scoliotic curve. The white spaces indicate absence of subjects in the considered level/degrees condition. Each normalized component is calculated as the ratio between the absolute value of the considered component and the sum of the absolute values of the three components.

However, such an approach is not expected to affect the evaluated outcomes since the contribution of the abdominal muscle can be considered as negligible in standing position. As commonly performed in spine musculoskeletal modelling, passive elements such as ligaments and facet joints were neglected, and the position of the intervertebral centers of rotation was kept fixed. Moreover, due to the lack of reference in vivo values in AIS, the joint moments (interpreting the role of the passive elements) were

assumed to be zero in the considered upright posture, considering the spinal segments to be in the neutral condition of the spine (Smit et al., 2011). However, stiffness-related reaction moments would only have occurred with induced segmental rotations. The rotatory muscles were not implemented, thus not allowing for predicting the contribution of the related torque, which could be associated with the axial rotation of the curve, considered by many clinicians a primary aspect of the deformity. Finally, muscle recruitment by central nervous system might be affected by scoliosis pathology, therefore muscle optimization method as used in typical musculoskeletal simulations of the healthy spine might be a source of limitation. Overall, according to the given explanations and to the structural peculiarities commonly assumed in the musculoskeletal modelling of the human spine, the reported limitations can be considered to have a minor influence, which does not compromise the validity of the results.

In conclusion, the study demonstrated the suitability of the spine model in replicating subject-specific scoliotic alignments. Trunk muscles were found more activated in the convex side of the scoliotic curve, in agreement with reference in vivo measurements, with progressive increase with scoliosis severity. The intervertebral lateral shear was found positively correlated with scoliosis severity, demonstrating that the transferred load is not a priori orthogonal to the vertebral endplate in the frontal plane, and thus questioning the assumption of the 'follower load' approach in case of experimental or computational study on the scoliotic spine. The computed biomechanical parameters can be exploited for clinical and computational applications, e.g., as potential predictors of the progression of the curve, and as inputs in numerical simulations based on finite element modelling.

Declaration of Competing Interest

The authors declare that they have no known competing financial interests or personal relationships that could have appeared to influence the work reported in this paper.

Acknowledgements

The study was partially supported by the Italian Ministry of Health (Ricerca Corrente).

References

Bassani, T., Galbusera, F., 2018. Chapter 15 - Musculoskeletal Modeling. Academic Press, pp. 257–277.

Bassani, T., Stucovitz, E., Galbusera, F., Brayda-Bruno, M., 2019. Is rasterstereography a valid noninvasive method for the screening of juvenile and adolescent idiopathic scoliosis?. European Spine Journal : Official Publication of the European Spine Society, the European Spinal Deformity Society, and the European Section of the Cervical Spine Research Society 28, 526–535.

Bassani, T., Galbusera, F., 2020. Statistics in experimental studies on the human spine: Theoretical basics and review of applications. Journal of the Mechanical Behavior of Biomedical Materials 110, 103862.

Been, E., Shefi, S., Kalichman, L., F Bailey, J., Soudack, M., 2018. Cross-sectional area of lumbar spinal muscles and vertebral endplates: a secondary analysis of 91 computed tomography images of children aged 2-20. Journal of Anatomy 233, 358-369.

Buttermann, G.R., Beaubien, B.P., 2008. In vitro disc pressure profiles below scoliosis fusion constructs. Spine 33, 2134–2142.

Cheung, J., Halbertsma, J.P., Veldhuizen, A.G., Sluiter, W.J., Maurits, N.M., Cool, J.C., van Horn, J.R., 2005. A preliminary study on electromyographic analysis of the paraspinal musculature in idiopathic scoliosis. European Spine Journal : Official Publication of the European Spine Society, the European Spinal Deformity Society, and the European Section of the Cervical Spine Research Society 14, 130–137.

Dao, T.T., 2016. RIGID MUSCULOSKELETAL MODELS OF THE HUMAN BODY SYSTEMS: A REVIEW. Journal of Musculoskeletal Research 19, 1630001.

de Sèze, M., Cugy, E., 2012. Pathogenesis of idiopathic scoliosis: a review. Annals of Physical and Rehabilitation Medicine 55, 128–138.

Dreischarf, M., Shirazi-Adl, A., Arjmand, N., Rohlmann, A., Schmidt, H., 2016. Estimation of loads on human lumbar spine: A review of in vivo and computational model studies. Journal of Biomechanics 49, 833–845.

Dreischarf, M., Zander, T., Bergmann, G., Rohlmann, A., 2010. A non-optimized follower load path may cause considerable intervertebral rotations. Journal of Biomechanics 43, 2625–2628.

Fong, D.Y., Lee, C.F., Cheung, K.M., Cheng, J.C., Ng, B.K., Lam, T.P., Mak, K.H., Yip, P.S., Luk, K.D., 2010. A meta-analysis of the clinical effectiveness of school scoliosis screening. Spine 35, 1061–1071.

Hachem, B., Aubin, C.E., Parent, S., 2017. Porcine spine finite element model: a complementary tool to experimental scoliosis fusionless instrumentation. European Spine Journal : Official Publication of the European Spine Society, the European Spinal Deformity Society, and the European Section of the Cervical Spine Research Society 26, 1610–1617.

Ignasiak, D., Dendorfer, S., Ferguson, S.J., 2016a. Thoracolumbar spine model with articulated ribcage for the prediction of dynamic spinal loading. Journal of Biomechanics 49, 959–966.

Ignasiak, D., Ferguson, S.J., Arjmand, N., 2016b. A rigid thorax assumption affects model loading predictions at the upper but not lower lumbar levels. Journal of Biomechanics 49, 3074–3078.

Illes, T., Somoskeoy, S., 2012. The EOS imaging system and its uses in daily orthopaedic practice. International Orthopaedics 36, 1325–1331.

Kwok, G., Yip, J., Cheung, M.C., Yick, K.L., 2015. Evaluation of Myoelectric Activity of Paraspinal Muscles in Adolescents with Idiopathic Scoliosis during Habitual Standing and Sitting. BioMed Research International 2015, 958450.

Lenke, L.G., Betz, R.R., Harms, J., Bridwell, K.H., Clements, D.H., Lowe, T.G., Blanke, K., 2001. Adolescent idiopathic scoliosis: a new classification to determine extent of spinal arthrodesis. The Journal of Bone and Joint Surgery. American 83, 1169– 1181.

Nnadi, C., Fairbank, J., 2010. Scoliosis: a review. Paediatr Child Health 20, 215–220.

Ovadia, D., 2013. Classification of adolescent idiopathic scoliosis (AIS). Journal of Children's Orthopaedics 7, 25–28.

Panjabi, M., Malcolmson, G., Teng, E., Tominaga, Y., Henderson, G., Serhan, H., 2007. Hybrid testing of lumbar CHARITE discs versus fusions. Spine 32, 959–966. discussion 967.

Patwardhan, A.G., Havey, R.M., Meade, K.P., Lee, B., Dunlap, B., 1999. A follower load increases the load-carrying capacity of the lumbar spine in compression. Spine 24, 1003–1009.

Rohlmann, A., Neller, S., Claes, L., Bergmann, G., Wilke, H.J., 2001. Influence of a follower load on intradiscal pressure and intersegmental rotation of the lumbar spine. Spine 26, E557–E561.

Rohlmann, A., Zander, T., Rao, M., Bergmann, G., 2009. Applying a follower load delivers realistic results for simulating standing. Journal of Biomechanics 42, 1520–1526.

Schlösser, T.P., van der Heijden, G.J., Versteeg, A.L., Castelein, R.M., 2014. How 'idiopathic' is adolescent idiopathic scoliosis? A systematic review on associated abnormalities. PloS One 9, e97461.

Schmid, S., Burkhart, K.A., Allaire, B.T., Grindle, D., Bassani, T., Galbusera, F., Anderson, D.E., 2020. Spinal Compressive Forces in Adolescent Idiopathic Scoliosis With and Without Carrying Loads: A Musculoskeletal Modeling Study. Frontiers in Bioengineering and Biotechnology 8, 159.

Smit, T.H., van Tunen, M.S., van der Veen, A.J., Kingma, I., van Dieën, J.H., 2011. Quantifying intervertebral disc mechanics: a new definition of the neutral zone. BMC Musculoskeletal Disorders 12. 38–2474-12-38.

Somoskeoy, S., Tunyogi-Csapo, M., Bogyo, C., Illes, T., 2012. Accuracy and reliability of coronal and sagittal spinal curvature data based on patient-specific threedimensional models created by the EOS 2D/3D imaging system. The Spine Journal : Official Journal of the North American Spine Society 12, 1052–1059.

Stokes, I.A., Spence, H., Aronsson, D.D., Kilmer, N., 1996. Mechanical modulation of vertebral body growth. Spine, 1162–1167.

Stokes, I.A., Gardner-Morse, M., 2004. Muscle activation strategies and symmetry of spinal loading in the lumbar spine with scoliosis. Spine 29, 2103–2107.

Weinstein, S.L., Dolan, L.A., Cheng, J.C., Danielsson, A., Morcuende, J.A., 2008. Adolescent idiopathic scoliosis. Lancet (London, England) 371, 1527–1537.

Wilke, H.J., Rohlmann, A., Neller, S., Graichen, F., Claes, L., Bergmann, G., 2003. ISSLS prize winner: A novel approach to determine trunk muscle forces during flexion and extension: a comparison of data from an in vitro experiment and in vivo measurements. Spine 28, 2585–2593.

Zapata, K.A., Wang-Price, S.S., Sucato, D.J., Dempsey-Robertson, M., 2015. Ultrasonographic measurements of paraspinal muscle thickness in adolescent idiopathic scoliosis: a comparison and reliability study. Pediatric Physical Therapy : The Official Publication of the Section on Pediatrics of the American Physical Therapy Association 27, 119–125.

Zoabli, G., Mathieu, P.A., Aubin, C.E., 2007. Back muscles biometry in adolescent idiopathic scoliosis. The Spine Journal : Official Journal of the North American Spine Society 7, 338–344.